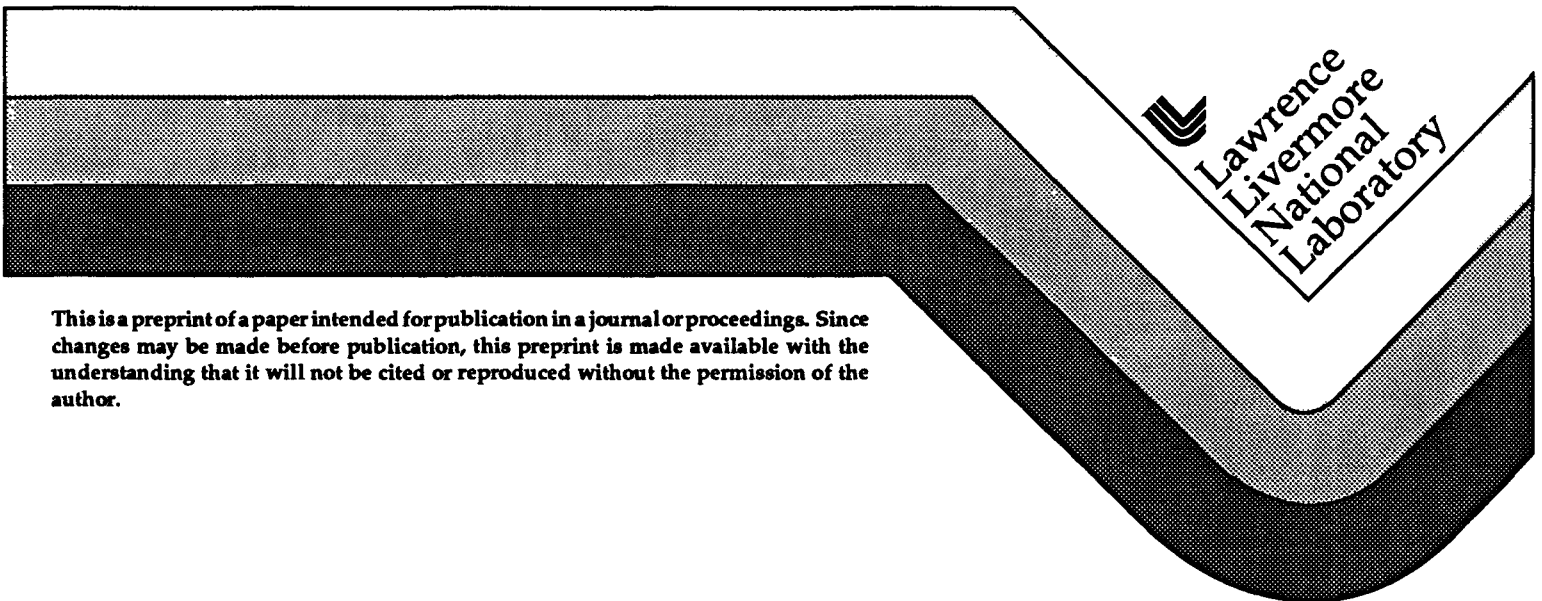


**Sputter Deposition of Multilayer Thermoelectric Films:
An Approach to the Fabrication of Two-Dimensional
Quantum Wells**

Joseph C. Farmer
Troy W. Barbee, Jr.
George C. Chapline, Jr.
Ronald J. Foreman
Leslie J. Summers
Mildred S. Dresselhaus
Lyndon D. Hicks

This paper was prepared for submittal to the
XIIIth International Conference on Thermoelectrics
Kansas City, MO
August 30-September 1, 1994

July 1994



This is a preprint of a paper intended for publication in a journal or proceedings. Since changes may be made before publication, this preprint is made available with the understanding that it will not be cited or reproduced without the permission of the author.

MASTER

DISTRIBUTION OF THIS DOCUMENT IS UNLIMITED

DISCLAIMER

Portions of this document may be illegible in electronic image products. Images are produced from the best available original document.

DISCLAIMER

This document was prepared as an account of work sponsored by an agency of the United States Government. Neither the United States Government nor the University of California nor any of their employees, makes any warranty, express or implied, or assumes any legal liability or responsibility for the accuracy, completeness, or usefulness of any information, apparatus, product, or process disclosed, or represents that its use would not infringe privately owned rights. Reference herein to any specific commercial products, process, or service by trade name, trademark, manufacturer, or otherwise, does not necessarily constitute or imply its endorsement, recommendation, or favoring by the United States Government or the University of California. The views and opinions of authors expressed herein do not necessarily state or reflect those of the United States Government or the University of California, and shall not be used for advertising or product endorsement purposes.

Sputter Deposition of Multilayer Thermoelectric Films: An Approach to the Fabrication of Two-Dimensional Quantum Wells

Joseph C. Farmer, Troy W. Barbee, Jr., George C. Chapline, Jr.,
Ronald J. Foreman, Leslie J. Summers,
Mildred S. Dresselhaus* and Lyndon D. Hicks*

*Chemistry and Materials Science Department
University of California
Lawrence Livermore National Laboratory
7000 East Avenue
Livermore, California 94550*

**Department of Physics
Massachusetts Institute of Technology
77 Massachusetts Avenue
Boston, Massachusetts 02139*

Abstract

The relative efficiency of a thermoelectric material is measured in terms of a dimensionless figure of merit, ZT . Though all known thermoelectric materials are believed to have $ZT \leq 1$, recent theoretical results predict that thermoelectric devices fabricated as two-dimensional quantum wells (2D QWs) or one-dimensional (1D) quantum wires could have $ZT \geq 3$. Multilayers with the dimensions of 2D QWs have been synthesized by alternately sputtering $\text{Bi}_{0.9}\text{Sb}_{0.1}$ and $\text{PbTe}_{0.8}\text{Se}_{0.2}$ onto a moving single-crystal sapphire substrate from dual magnetrons. These materials have been used to test the thermoelectric quantum-well concept and gain insight into relevant transport mechanisms. If successful, this research could lead to thermoelectric devices that have efficiencies close to that of an ideal Carnot engine. Ultimately, such devices could be used to replace conventional heat engines and mechanical refrigeration systems.

Background

Introduction. The relative efficiency of a thermoelectric material is measured in terms of the dimensionless figure of merit, ZT . The best known thermoelectric materials are heavily doped, mildly degenerate semiconductors and have $ZT \leq 1$. If materials with $ZT \geq 3$ could be found or developed, thermoelectric devices could be made that would have thermodynamic efficiencies close to that of an ideal Carnot

engine. In fact, such materials would make it possible to completely replace conventional heat engines and mechanical chlorofluorocarbon (CFC) refrigeration systems with solid state devices. Conventional thermoelectric materials ($ZT \leq 1$) are used in nuclear-fueled power sources for space exploration, in silent power sources for the military, and in solid-state electrical generators on diesel engines. Given the environmental problems associated with CFC refrigeration and air conditioning, the demand for efficient solid-state alternatives should be great. High-efficiency thermoelectric coolers could also be used to eliminate evaporative losses from storage systems for liquefied nitrogen, oxygen, and hydrogen. Conventional thermoelectric devices are now used to cool infrared detectors, integrated circuits, food and beverages for long-distance truck drivers, the bodies of pilots and soldiers involved in desert and chemical warfare, and passenger compartments in electric trains. We are pursuing the development of 2D QWs as a means of achieving high ZT . Theory predicts that thermoelectric devices fabricated as 2D QWs could have $ZT \geq 3$.

Figure of merit determines efficiency. The thermodynamic efficiency of a thermoelectric power generator (η) and the coefficient of performance (β or COP) of a Peltier cooler are both calculated from the dimensionless figure of merit (ZT). The coefficient of performance is defined as the ratio of cooling to electrical power. Expressions for η and β at optimum current levels are

$$\eta = \frac{T_h - T_c}{T_h} \frac{\sqrt{1 + ZT} - 1}{\sqrt{1 + ZT} + T_c / T_h} \quad (1)$$

$$\beta = \frac{T_c}{T_h - T_c} \frac{\sqrt{1+ZT} - T_h/T_c}{\sqrt{1+ZT} + 1} \quad (2)$$

where T_h is the temperature of the hot side of the device and T_c is the temperature of the cold side [1,2]. To achieve high values of η or β with a thermoelectric device, a material with a large ZT value must be found [3].

Conventional Strategies for Maximizing ZT. The dimensionless figure of merit, ZT, is determined by the Seebeck coefficient (α), electrical conductivity (σ), electronic thermal conductivity (κ_{el}), and lattice thermal conductivity (κ_{ph}).

$$ZT = \frac{\sigma \alpha^2}{\kappa_{ph} + \kappa_{el}} T \quad (3)$$

Good thermoelectric materials should have large Seebeck coefficients (α), large electrical conductivities (σ), and small thermal conductivities ($\kappa_{ph} + \kappa_{el}$). Mildly degenerate semiconductors have the best combinations of these intrinsic properties [4]. Unfortunately, attempts to improve ZT by increasing σ are eventually counteracted by detrimental changes in κ_{el} . The Wiedemann-Franz law requires that σ and κ_{el} trend in the same direction. Since α , σ , and κ_{el} are all sensitive to carrier concentration, ZT is optimized by changing the extent of doping. The optimum is usually in the vicinity of 10^{19} cm^{-3} . It is also desirable for thermoelectric materials to have low lattice thermal conductivities (κ_{ph}). Semiconductor compounds made from elements with high atomic mass tend to have lower κ_{ph} than those made from lighter elements.

Theoretical Basis for Thermoelectric Multilayer Films

2D QW Model Predicts $ZT \geq 3$. From reviewing published data, we have concluded that no dramatic improvement in the dimensionless figure of merit, i.e. $ZT \gg 1$, has been achieved during the past thirty years. However, Hicks and Dresselhaus of MIT have recently developed a model for the thermoelectric properties of 2D QWs, which has led to some promising predictions [5-8]. In bulk form, $\text{Bi}_{0.9}\text{Sb}_{0.1}$ is a narrow-band semiconductor. This results in conduction by both electrons and holes. In this case, ZT is reduced from the value it would have if the conduction were by the conduction or valence band alone. Quantum confinement of $\text{Bi}_{0.9}\text{Sb}_{0.1}$ should increase the band gap separating the electrons and holes, thereby increasing ZT. This superlattice behaves like a single-band 2D QW. The Seebeck coefficient, electrical conductivity, and electronic contribution to the thermal conductivity of the 2D QW are derived from the electronic dispersion relationship for motion confined in the lowest sub-band of the 2D QW and are given as follows:

$$\alpha = -\frac{k_B}{e} \left(\frac{2F_1}{F_0} - \zeta^* \right) \quad (4)$$

$$\sigma = \frac{1}{2\pi a} \left(\frac{2k_B T}{\hbar^2} \right) (m_x m_y)^{\frac{1}{2}} F_0 e \mu_x \quad (5)$$

$$\kappa_{el} = \frac{\tau \hbar^2}{4\pi a} \left(\frac{2k_B T}{\hbar^2} \right)^2 \left(\frac{m_y}{m_x} \right)^{\frac{1}{2}} k_B \left(3F_2 - \frac{4F_1^2}{F_0} \right) \quad (6)$$

where k_B is Boltzmann's constant, F_λ is the Fermi-Dirac integral, e is the electronic charge, T is temperature, m_x is the mobility in the x-direction, τ is the relaxation time, and ζ^* is the reduced chemical potential relative to the edge of the conduction band (Fermi energy level) and is defined as:

$$\zeta^* = \frac{\zeta - \frac{\hbar^2 \pi^2}{2m_x a^2}}{k_B T} \quad (7)$$

The Fermi-Dirac integral is given by:

$$F_\lambda = F_\lambda(\zeta^*) = \int_0^\infty \frac{x^\lambda dx}{e^{(x-\zeta^*)} + 1} \quad (8)$$

Fermi-Dirac transport integrals have different values, depending on whether they are calculated with ζ^* for 2D or 3D. The dimensionless figure of merit for a 2D material is:

$$ZT_{2D} = \frac{\left(\frac{2F_1}{F_0} - \zeta^* \right)^2 F_0}{\frac{1}{B} + 3F_2 - \frac{4F_1^2}{F_0}} \quad (9)$$

where the parameter B accounts for the phonon contribution to the thermal conductivity. This parameter is defined by Eq. 10.

$$B = \frac{1}{2\pi a} \left(\frac{2k_B T}{\hbar^2} \right) (m_x m_y)^{\frac{1}{2}} \frac{k_B^2 T \mu_x}{e \kappa_{ph}} \quad (10)$$

Note that ZT_{2D} may be varied both by changing doping and changing the $\text{Bi}_{0.9}\text{Sb}_{0.1}$ layer thickness. A prediction of ZT for the $\text{Bi}_{0.9}\text{Sb}_{0.1}/\text{PbTe}_{0.8}\text{Se}_{0.2}$ system as a function of layer thickness was made with the Hicks-Dresselhaus model, assuming optimum doping, and is shown in Fig. 1.

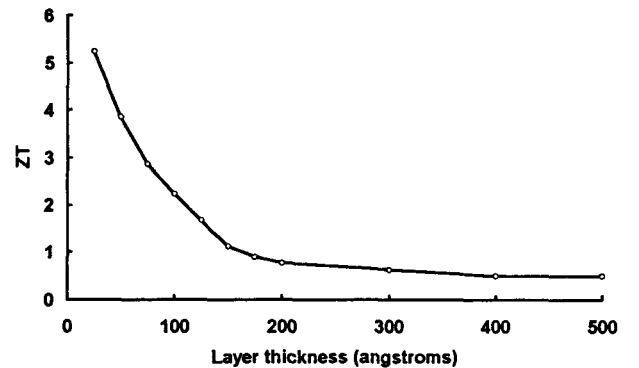


Figure 1. Predicted ZT_{2D} for $\text{Bi}_{0.9}\text{Sb}_{0.1}/\text{PbTe}_{0.8}\text{Se}_{0.2}$ layer pairs as a function of thickness.

In this case, quantum theory indicates that it should be possible to achieve $ZT \geq 3$ with relatively thick $\text{Bi}_{0.9}\text{Sb}_{0.1}$ layers (approximately 75 angstroms). Harman, also of MIT, has used MBE to make short-period superlattices of $\text{Bi}_{0.9}\text{Sb}_{0.1}$ and $\text{PbTe}_{0.8}\text{Se}_{0.2}$ [9]. He has produced multilayer structures with

up to 4000 monolayers and "encouraging" thermoelectric properties.

Confirmation of Quantum Well Model. Measurements of electrical conductivity alone should be sufficient to confirm the predicted QW behavior, provided that the carrier density is in the proper range. From Hicks and Dresselhaus, we know that the ratio of the 2D and 3D electrical conductivities is:

$$\frac{\sigma_{2D}}{\sigma_{3D}} = \frac{\pi F_{0,2D}}{a F_{1/2,3D}} \frac{\hbar}{\sqrt{2m_e k_B T}} \quad (11)$$

From this ratio, we find that the critical dimension for QW enhancement of the electrical conductivity is:

$$a \leq \pi \frac{F_{0,2D}}{F_{1/2,3D}} \frac{\hbar}{\sqrt{2m_e k_B T}} \quad (12)$$

The Hicks-Dresselhaus model predicts that the electrical conductivity should increase as the width of the QW, a , is decreased. If we observe that σ_{2D}/σ_{3D} has such a dependence, we will have at least a partial confirmation of the theory, as well as evidence that the multilayer thermoelectric film is exhibiting QW behavior. A more complete confirmation can be done if the Seebeck coefficient is known. Hicks and Dresselhaus also give theoretical expressions for both α_{2D} and α_{3D} . These expressions and those for the 2D and 3D electrical conductivities can be used to predict the QW enhancement of the thermoelectric power factor, $\sigma\alpha^2$.

$$\frac{\sigma_{2D}\alpha_{2D}^2}{\sigma_{3D}\alpha_{3D}^2} = \frac{\pi F_{0,2D}}{a F_{1/2,3D}} \frac{\hbar}{\sqrt{2m_e k_B T}} \left(\frac{2F_{1,2D} - \zeta_{2D}}{F_{0,2D}} - \frac{5F_{3/2,3D} - \zeta_{3D}}{3F_{1/2,3D}} \right)^2 \quad (13)$$

Usually, high power factors ($\sigma\alpha^2$) are indicative of good thermoelectric materials. If we could determine the thermal conductivity, $\kappa_{el} + \kappa_{ph}$, the figure of merit, Z , could be calculated. However, it is important to note that both the theory and material can be tested without measurement of the thermal conductivity.

Needed Improvements in Theory. The original theory developed by Hicks and Dresselhaus for 2D QW shows the advantage of QW thermoelectric devices, but does not account for the scattering of charge carriers by defects, impurities, rough interfaces, and phonons. The model also fails to account for the trapping of charge carriers. These deficiencies are recognized and deserve the attention of theoretical solid-state physicists. Data presented here should facilitate the development of more complete theories.

Technique for Synthesizing Multilayer Thermoelectric Films

A Practical Approach to Synthesis. MBE is believed to be too expensive for the production of practical thermoelectric materials. However, sputtering, which is more than two orders of magnitude faster, has been demonstrated to allow fabrication of high-quality films and multilayers with QW dimensions [10-13]. Here, for the first time, we report the sputter deposition of

Bi_{0.9}Sb_{0.1}/PbTe_{0.8}Se_{0.2} multilayer films with the dimensions of 2D QWs. Bi_{0.9}Sb_{0.1} quantum wells are predicted to have much better thermoelectric performance than those made of other thermoelectric materials such as Bi₂Te₃. The effects of substrate temperature on the structure and orientation of deposited layers has been investigated. The Seebeck coefficient, electrical conductivity, thermal conductivity, and dimensionless figure of merit of each film have been determined as functions of temperature (ambient to 250°C) by the techniques described in a subsequent section. These measurements were made in an attempt to verify the Hicks-Dresselhaus model.

Details of the Sputtering Process. Multilayer thermoelectric films (2D QWs) are synthesized by sputtering onto a moving substrate from dual magnetrons. The quantum-well (QW) layer is sandwiched between two barrier layers. Typically, the QW material has a very narrow band gap and the barrier material has a relatively large band gap. Sputtering is done in a novel system that was developed for the fabrication of X-ray optics. Vacuum is established and maintained by a two-stage mechanical roughing pump and a high-capacity cryogenic pump. The system usually achieves base pressures of approximately 10⁻⁸ torr after bake-out and before sputtering. Substrates are mounted on a rotating carousel driven by a precision stepper motor. Substrates can be heated or cooled by the carousel during sputtering. Heating of the substrate during deposition and subsequent annealing is used as means of controlling the structure and orientation of individual crystalline layers, as well as means of reducing the number of defects in films. One of the essential conditions for epitaxial film growth is a high mobility of condensed atoms and molecules on the surface of the substrate. Since mobility depends upon kinetic energy, it is desirable to heat the substrate during deposition. Two 1 kW magnetrons, each having a 2.5-inch diameter target and a 1 kW power supply, are used to deposit films. The sputter sources are operated at an argon pressure between 0.001 and 0.1 torr. Argon is admitted to the system by a precision flow controller. All functions of the system, including movement of the carousel, rates of heating and cooling, magnetron power, and argon pressure, are computer controlled.

Techniques for Characterizing Thermoelectric Thin Films

Structural Characterization. X-ray fluorescence (XRF) is used to verify the composition of sputtering targets while X-ray diffraction (XRD) is used to verify their crystal structure. Transmission electron microscopy (TEM) with selected-area transmission electron diffraction is used to determine characteristics of single-layer, bilayer, and multilayer thermoelectric films such as crystallographic orientation and thickness of individual layers. Auger electron spectroscopy (AES) with depth profiling is used to study compositional variations across interfaces. Results are discussed in a subsequent section.

Seebeck Coefficient. The Seebeck coefficient, electrical conductivity, and power factor of all thin films are determined as functions of temperature. Since these films are supported by a substrate and cannot be thermally isolated, the standard Harman technique cannot be used. Instead, the Seebeck

coefficient is determined with a differential hot stage. One end of the film is heated while the opposite end is cooled. During the first phase of the experiment, Stage No. 1 serves as the heat sink while Stage No. 2 serves as the heat source, thereby producing a positive temperature gradient. During the second phase of the experiment, Stage No. 1 serves as the heat source while Stage No. 2 serves as the heat sink, thereby producing a negative temperature gradient. The film is electrically isolated from the two stages by the sapphire substrate. The Seebeck coefficient is estimated from the temperature difference, ΔT , and the voltage difference, ΔV .

$$\alpha = -\frac{\Delta V}{\Delta T} \quad (14)$$

This approach has been applied to a number of single-layer, bilayer, and multilayer $\text{Bi}_{0.9}\text{Sb}_{0.1}/\text{PbTe}_{0.8}\text{Se}_{0.2}$ films. For example, the Seebeck coefficient of a single-layer $\text{PbTe}_{0.8}\text{Se}_{0.2}$ film having a thickness of approximately 7,900 angstroms was determined. The temperature profiles and the corresponding differential voltage are shown in Figs. 2 and 3, respectively. Results are discussed in a subsequent section.

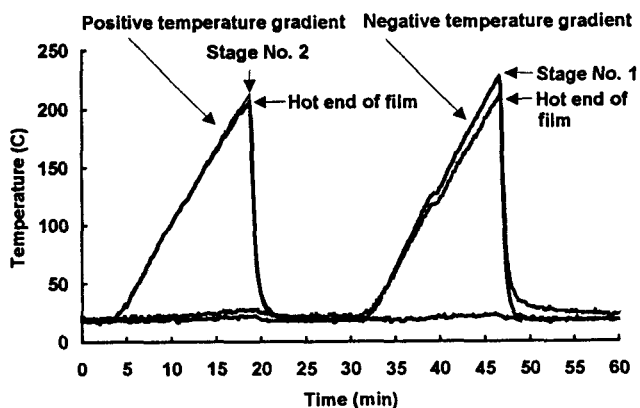


Figure 2. Temperature profiles of the differential hot stage during measurement the Seebeck coefficient of a single-layer $\text{PbTe}_{0.8}\text{Se}_{0.2}$ film with a thickness of 7,900 angstroms. The corresponding differential voltage is shown in Fig. 3.

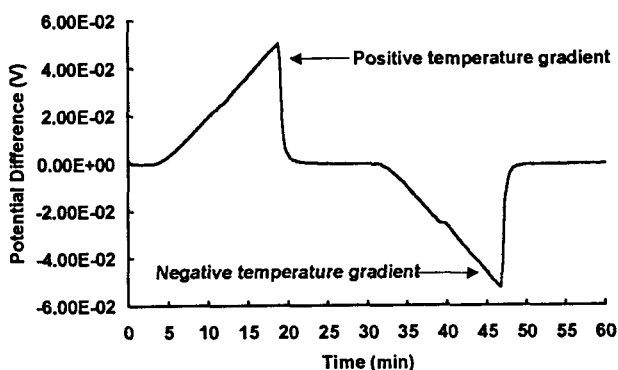


Figure 3. Potential difference due to temperature gradients shown in Fig. 2.

Electrical conductivity. Variations of ASTM Standards F43 and F46 are used to evaluate these novel thin films. The samples are configured in accordance with the two-probe method. First, a precision resistor is connected in series with the thin film. Then, a bipolar potential pulse is applied across the terminals of the resistor by an adder potentiostat. This causes a corresponding current pulse, I_{pulse} , to flow through the resistor and the thin film simultaneously. Two spring-loaded probes and one channel of a two-channel digital oscilloscope are used to measure the potential drop, V_{pulse} , over a known length of film, L . This potential drop is also monitored with a lock-in amplifier. To assure reliability of the results, the second channel of the oscilloscope is used to monitor the 100 mV differential across the resistor. The electrical conductivity, σ , is calculated directly from the ratio of the amplitudes of I_{pulse} and V_{pulse} .

$$\sigma = \frac{L}{WH} \frac{I_{\text{pulse}}}{V_{\text{pulse}}} \quad (15)$$

where W and H are the width and thickness of the film, respectively. The reliability of this experimental technique has been checked by evaluating several metallic films. For example, the resistivities ($\rho=1/\sigma$) of several sputtered copper films were determined at ambient temperature and found to be in the range of 1.80 to 2.32 $\mu\Omega\text{-cm}$. These measurements compare reasonably well to a published value of 1.77 $\mu\Omega\text{-cm}$ for crystalline copper. Results for $\text{Bi}_{0.9}\text{Sb}_{0.1}/\text{PbTe}_{0.8}\text{Se}_{0.2}$ films are discussed in a subsequent section.

Results with $\text{Bi}_{0.9}\text{Sb}_{0.1}/\text{PbTe}_{0.8}\text{Se}_{0.2}$ on Sapphire

Synthesis of $\text{Bi}_{0.9}\text{Sb}_{0.1}/\text{PbTe}_{0.8}\text{Se}_{0.2}$ 2D QWs. The Hicks-Dresselhaus model for two-dimensional quantum wells predicts that an exceptional ZT should be achievable with 75 angstrom layers of $\text{Bi}_{0.9}\text{Sb}_{0.1}$ separated by $\text{PbTe}_{0.8}\text{Se}_{0.2}$ barrier. Good progress has been made towards synthesizing such $\text{Bi}_{0.9}\text{Sb}_{0.1}/\text{PbTe}_{0.8}\text{Se}_{0.2}$ multilayer films on single-crystal silicon (100) and sapphire (1102) substrates. Substrates were either maintained at ambient temperature or heated to approximately 35% of the melting point of the film. Results with sapphire substrates are reported here. We have demonstrated that we can make $\text{Bi}_{0.9}\text{Sb}_{0.1}$ and $\text{PbTe}_{0.8}\text{Se}_{0.2}$ single-layer films, as well as $\text{Bi}_{0.9}\text{Sb}_{0.1}/\text{PbTe}_{0.8}\text{Se}_{0.2}$ bilayer and multilayer films with $\text{Bi}_{0.9}\text{Sb}_{0.1}$ layers less than 75 angstroms thick. The abrupt compositional change at the $\text{Bi}_{0.9}\text{Sb}_{0.1}$ - $\text{PbTe}_{0.8}\text{Se}_{0.2}$ interface has been verified by AES with depth profiling. Structural analyses have been done with TEM and XRD. Columnar growth is evident. Such growth is common in sputtered single-layer films, but is surprising in sputtered multilayers. Well-defined individual layers of $\text{Bi}_{0.9}\text{Sb}_{0.1}$ and $\text{PbTe}_{0.8}\text{Se}_{0.2}$ are continuous and extend across virtually all columnar crystals. It is surprising that the interface between individual layers did not interrupt columnar growth. A typical columnar crystal has a characteristic lateral dimension (dimension parallel to film-substrate interface) of 1000-3000 angstroms. Despite the scattering of charge carriers by defects and interfaces between these columnar crystals, we believe that it should be possible to achieve some degree of

quantum-well confinement in such films. Thermoelectric properties of these single-layer, bilayer, and multilayer films have been determined over a temperature range extending from ambient up to 250°C.

Resistivity Measurements. A single-layer film of $\text{Bi}_{0.9}\text{Sb}_{0.1}$ with a thickness of 8,800 angstroms was deposited on single-crystal sapphire maintained at ambient temperature. This film was too thick to exhibit any of the characteristics of a 2D QW. Resistivity measurements were made while cycling the sample between ambient temperature and approximately 190°C. As shown in Fig. 4, the resistivity of this relatively thick film dropped from 9.2 m Ω -cm at ambient temperature to 7.1 m Ω -cm at approximately 150°C. The resistivity returned to the original value after cooling.

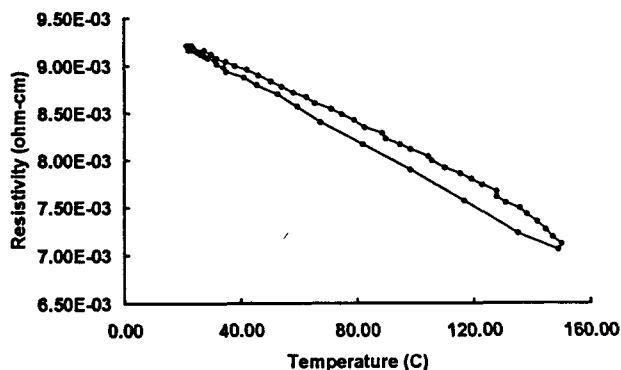


Figure 4. Resistivity of single-layer films of $\text{Bi}_{0.9}\text{Sb}_{0.1}$ having a thickness of 8,800 angstroms.

Recently, the thermoelectric properties of extruded and single-crystal $\text{Bi}_{0.91}\text{Sb}_{0.01}$ alloys were published by Sidorenko and Mosalon [14]. Unfortunately, they provide no data for the temperature range shown in Fig. 4. However, they give a representative resistivity of approximately 0.1 m Ω -cm at 200 K (-73°C). By extrapolating the data shown in Fig. 4 down to 200 K, we conclude that sputtered single-layer films of $\text{Bi}_{0.9}\text{Sb}_{0.1}$ are not as conductive as bulk single crystals. The relatively high resistivity of the sputtered film may be due to a greater degree of disorder. It may also be due to the formation of oxides in the film. Note that the films are exposed to air during transfer from the sputtering system to the environmental chamber where electronic measurements are made. Since thermal cycling does not increase the resistivity, we conclude that no deterioration of the film occurs during such electronic characterization. Additional work is being done to assess the extent of oxidation in these single-layer $\text{Bi}_{0.9}\text{Sb}_{0.1}$ films during sample transfer. Due to this uncertainty, we cannot determine whether or not such sputtered films can be used as the basis of synthesizing 2D QWs.

A film of $\text{PbTe}_{0.8}\text{Se}_{0.2}$ having a thickness of approximately 26,000 angstroms was deposited on single-crystal sapphire maintained at ambient temperature. Resistivity measurements were made while cycling the sample between ambient temperature and approximately 190°C. As shown in Fig. 5, the resistivity of this film dropped from 3 Ω -cm at ambient temperature to 0.5 Ω -cm at approximately 190°C.

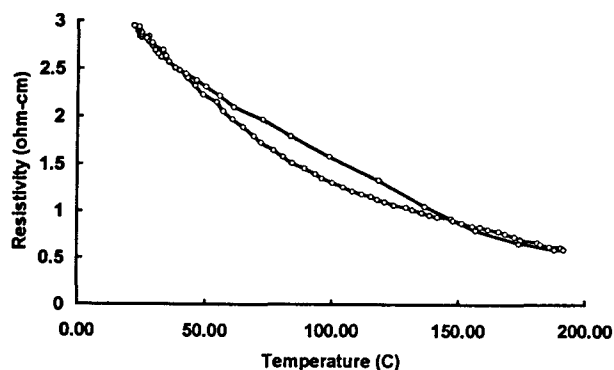


Figure 5. Resistivity of single-layer films of $\text{PbTe}_{0.8}\text{Se}_{0.2}$ having a thickness of approximately 26,000 angstroms.

The resistivity of undoped $\text{PbTe}_{0.8}\text{Se}_{0.2}$ is three orders of magnitude greater than the resistivity of $\text{Bi}_{0.9}\text{Sb}_{0.1}$. These thick $\text{PbTe}_{0.8}\text{Se}_{0.2}$ films have sufficiently high resistivities and stabilities to qualify them as candidate barrier layers for $\text{Bi}_{0.9}\text{Sb}_{0.1}$ quantum wells.

Thinner single-layer films of $\text{PbTe}_{0.8}\text{Se}_{0.2}$ with thicknesses of only 7,900 angstroms were also deposited onto ambient-temperature, single-crystal sapphire. Resistivity measurements were made while cycling the sample between ambient and approximately 150°C. As shown in Fig. 6, the resistivity of this relatively thin film dropped from 1.7 Ω -cm at ambient temperature to less than 0.5 Ω -cm at approximately 150°C.

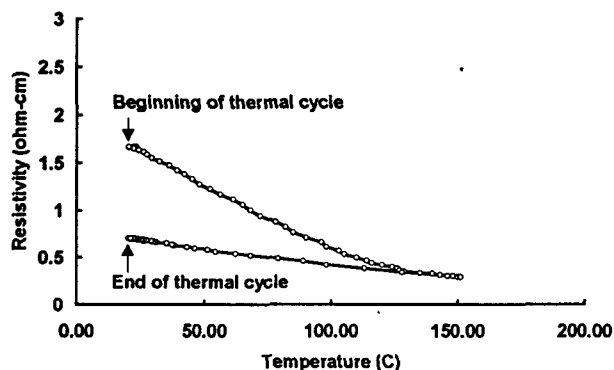


Figure 6. Resistivity of single-layer films of $\text{PbTe}_{0.8}\text{Se}_{0.2}$ having a thickness of 7,900 angstroms.

The ambient temperature resistivity of the film at the end of the cycle was about 0.7 Ω -cm. In this case, thermal cycling enhanced the conductivity, probably by reducing the number of defects in film. Such irreversibility raises concern about the structural stability of this candidate barrier material at elevated temperature. In this context, an elevated temperature is defined as any temperature greater than that at which the film was deposited.

Bilayer films of $\text{Bi}_{0.9}\text{Sb}_{0.1}$ and $\text{PbTe}_{0.8}\text{Se}_{0.2}$ were made by first depositing 6,500 angstroms of $\text{Bi}_{0.9}\text{Sb}_{0.1}$ directly onto ambient-temperature, single-crystal sapphire and subsequently depositing 400 angstroms of $\text{PbTe}_{0.8}\text{Se}_{0.2}$ onto the $\text{Bi}_{0.9}\text{Sb}_{0.1}$ layer. Resistivity measurements were been made over a range

extending from ambient temperature to approximately 160°C, as illustrated by Fig. 7.

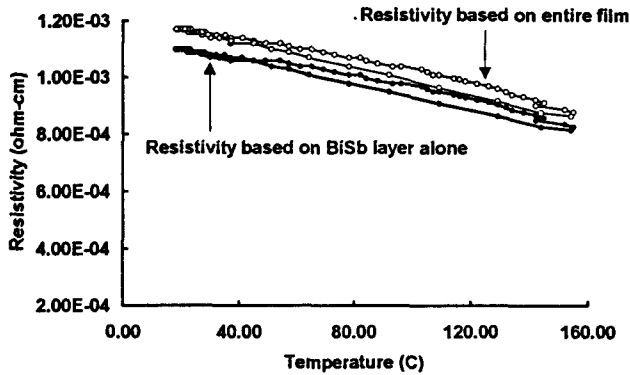


Figure 7. Resistivity of bilayer film consisting of 6,500 angstroms of $\text{Bi}_{0.9}\text{Sb}_{0.1}$ and 400 angstroms of $\text{PbTe}_{0.8}\text{Se}_{0.2}$.

The resistivity based on the entire film, assuming conduction in both layers, dropped from 1.2 mΩ-cm at ambient temperature to 0.90 mΩ-cm at 160°C. From the data shown in Figs. 4, 5, and 6, we conclude that conduction in undoped $\text{PbTe}_{0.8}\text{Se}_{0.2}$ layers should be negligible compared to conduction in the $\text{Bi}_{0.9}\text{Sb}_{0.1}$ layers. As shown in Fig. 7, the resistivity based on the $\text{Bi}_{0.9}\text{Sb}_{0.1}$ layer alone dropped from 1.1 mΩ-cm at ambient temperature to 0.85 mΩ-cm at 160°C. From this data we also conclude that thick $\text{Bi}_{0.9}\text{Sb}_{0.1}/\text{PbTe}_{0.8}\text{Se}_{0.2}$ bilayers have much better conductivity than single-layer films of either $\text{Bi}_{0.9}\text{Sb}_{0.1}$ or $\text{PbTe}_{0.8}\text{Se}_{0.2}$. In the case of bilayer films, we believe that the $\text{PbTe}_{0.8}\text{Se}_{0.2}$ cap, which is thermodynamically stable in air, prevents oxidation of the underlying $\text{Bi}_{0.9}\text{Sb}_{0.1}$ layer during sample transfer. Consequently, good electrical conductivity is maintained. However, we also recognize that some enhancement in conductivity could be due to the doping of $\text{Bi}_{0.9}\text{Sb}_{0.1}$ by $\text{PbTe}_{0.8}\text{Se}_{0.2}$, or the doping of $\text{PbTe}_{0.8}\text{Se}_{0.2}$ by $\text{Bi}_{0.9}\text{Sb}_{0.1}$. In this case, the individual layers are too thick for any enhancement due to quantum-well confinement. No irreversibility was observed while cycling the temperature. Much thinner bilayer films were made by depositing 64 Angstroms of $\text{Bi}_{0.9}\text{Sb}_{0.1}$ and 115 Angstroms of $\text{PbTe}_{0.8}\text{Se}_{0.2}$ onto ambient-temperature, single-crystal sapphire. Resistivity data for these films are shown in Fig. 8.

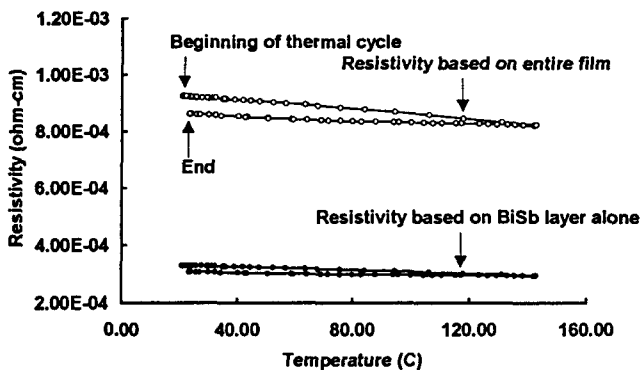


Figure 8. Resistivity of bilayer film consisting of 64 angstroms of $\text{Bi}_{0.9}\text{Sb}_{0.1}$ and 115 angstroms of $\text{PbTe}_{0.8}\text{Se}_{0.2}$.

In this case, enhanced conductivity of the $\text{Bi}_{0.9}\text{Sb}_{0.1}$ layer is correlated with reduced dimensionality and may be due to quantum-well confinement. The profound impact of such

effects at a layer thickness of only 64 angstroms is illustrated by the theoretical predictions shown in Fig. 1. Enhanced conductivity of the $\text{Bi}_{0.9}\text{Sb}_{0.1}$ layer may also be due to ambipolar doping by the $\text{PbTe}_{0.8}\text{Se}_{0.2}$ layer, as well as unexpected conduction in the $\text{PbTe}_{0.8}\text{Se}_{0.2}$ layer due to unintentional doping. Temperature cycling degrades conductivity slightly, possibly due to enhanced interdiffusion of layers.

Multilayer films were made by depositing alternating layers of $\text{Bi}_{0.9}\text{Sb}_{0.1}$ and $\text{PbTe}_{0.8}\text{Se}_{0.2}$ onto ambient-temperature, single-crystal sapphire substrates. Layers of $\text{Bi}_{0.9}\text{Sb}_{0.1}$ were 143 angstroms thick, layers of $\text{PbTe}_{0.8}\text{Se}_{0.2}$ were 115 angstroms thick, and the entire film was approximately 17,000 angstroms thick. From the data shown in Fig. 9, it is evident that reduced dimensionality also improves the conductivity of $\text{Bi}_{0.9}\text{Sb}_{0.1}$ incorporated into multilayer films.

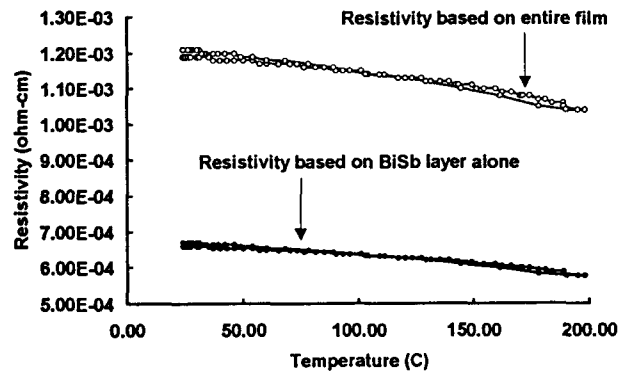


Figure 9. Resistivity of multilayer film consisting of alternating layers of $\text{Bi}_{0.9}\text{Sb}_{0.1}$ and $\text{PbTe}_{0.8}\text{Se}_{0.2}$ on a single-crystal sapphire substrate.

Here too the improvement may be due to either quantum-well confinement or unexpected doping effects.

Seebeck Coefficient Measurements. The differential hot stage described in a previous section was used to determine Seebeck coefficients of thermoelectric thin films by imposing temperature gradients and measuring differential voltages. Data for a single-layer film of $\text{Bi}_{0.9}\text{Sb}_{0.1}$ with a thickness of 8,800 angstroms and deposited on a single-crystal sapphire substrate maintained at ambient temperature are shown below.

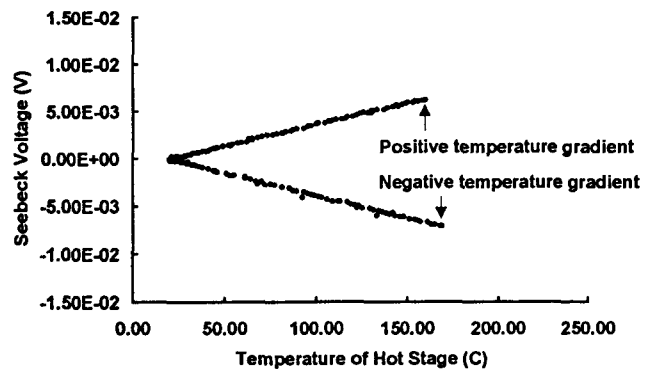


Figure 10. Seebeck voltage of single-layer films of $\text{Bi}_{0.9}\text{Sb}_{0.1}$ having a thickness of 8,800 angstroms. The temperature of the cold stage was maintained at approximately 20°C.

Since the single-crystal sapphire substrate was completely insulating it did not contribute to the observed Seebeck voltage.

While imposing the positive temperature gradient, the average Seebeck coefficient of this n-type material was determined to be $-45 \mu\text{V/K}$. While imposing the negative temperature gradient, a value of $-47 \mu\text{V/K}$ was determined. As expected, the two measurements are in close agreement (within 4%). As previously discussed, Sidorenko and Molsolon have published thermoelectric properties of extruded and single-crystal $\text{Bi}_{0.91}\text{Sb}_{0.09}$ alloys [14]. A representative Seebeck coefficient for these bulk materials is slightly less than $-100 \mu\text{V/K}$ at 200K, which is about twice the average value reported here for a sputtered single-layer film between ambient temperature and 160°C . Recall that the resistivity measurements of this film were shown in Fig. 4.

As shown in Fig. 11, an imposed temperature gradient was also used to produce the observed Seebeck voltage in a single-layer $\text{PbTe}_{0.8}\text{Se}_{0.2}$ film, which had a thickness of 26,000 angstroms.

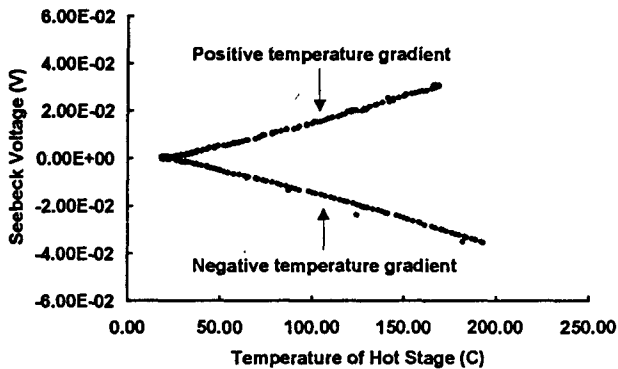


Figure 11. Seebeck voltage of single-layer films of $\text{PbTe}_{0.8}\text{Se}_{0.2}$ having a thickness of 26,000 angstroms. The temperature of the cold stage was maintained at approximately 20°C .

The average Seebeck coefficient was determined from the slope of the voltage-temperature curve and is approximately $-190 \mu\text{V/K}$. The negative Seebeck coefficient indicates that the film is n-type. The corresponding resistivity measurement for this film is shown in Fig. 5. This single-layer film is a n-type semiconductor. The Seebeck voltage of a thinner $\text{PbTe}_{0.8}\text{Se}_{0.2}$ film deposited under the same conditions and having a thickness of only 7,900 angstroms is shown in Fig. 12.

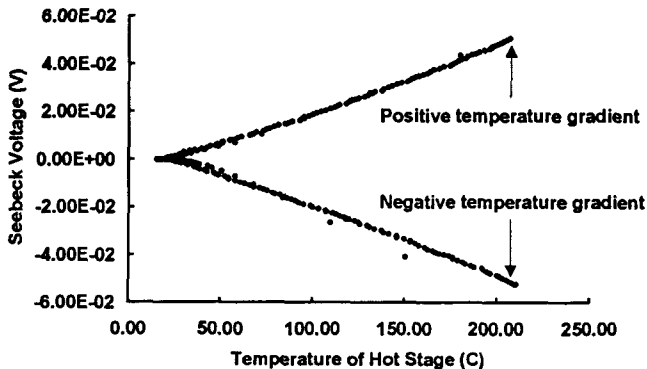


Figure 12. Seebeck voltage of single-layer films of $\text{PbTe}_{0.8}\text{Se}_{0.2}$ having a thickness of 7,900 angstroms. The temperature of the cold stage was maintained at approximately 20°C .

In this case, the average Seebeck coefficient was determined to be approximately $-230 \mu\text{V/K}$, which is similar to that of the thicker film. The corresponding resistivity measurement is shown in Fig. 6. Though temperature cycling changed the resistivity slightly, it had no noticeable effect on the Seebeck coefficient. The Seebeck voltage of a bilayer film consisting of 6,500 angstroms of $\text{Bi}_{0.9}\text{Sb}_{0.1}$ and 400 Angstroms of $\text{PbTe}_{0.8}\text{Se}_{0.2}$ deposited onto ambient-temperature, single-crystal sapphire is shown in Fig. 13.

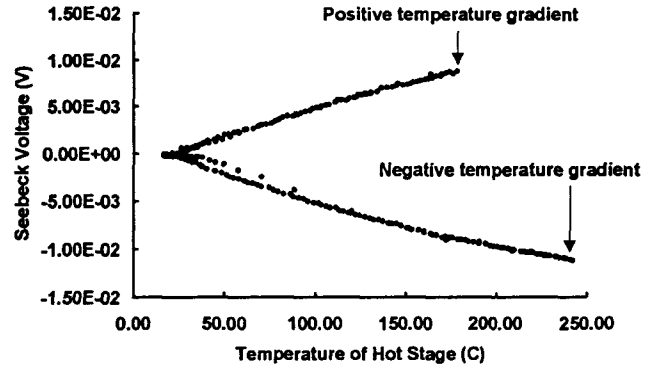


Figure 13. Seebeck voltage of bilayer film consisting of 6,500 angstroms of $\text{Bi}_{0.9}\text{Sb}_{0.1}$ and 400 angstroms of $\text{PbTe}_{0.8}\text{Se}_{0.2}$. The temperature of the cold stage was maintained at approximately 20°C .

The average Seebeck coefficient is approximately $-60 \mu\text{V/K}$, which is considerably less than that of a $\text{PbTe}_{0.8}\text{Se}_{0.2}$ single-layer film. However, it is slightly greater than that of a single-layer $\text{Bi}_{0.9}\text{Sb}_{0.1}$ film. Recall that the corresponding Seebeck coefficient of uncapped $\text{Bi}_{0.9}\text{Sb}_{0.1}$ is approximately $-45 \mu\text{V/K}$. The Seebeck voltage of a bilayer consisting of 64 angstroms of $\text{Bi}_{0.9}\text{Sb}_{0.1}$ and 115 angstroms of $\text{PbTe}_{0.8}\text{Se}_{0.2}$ deposited under identical conditions is shown in Fig. 14.

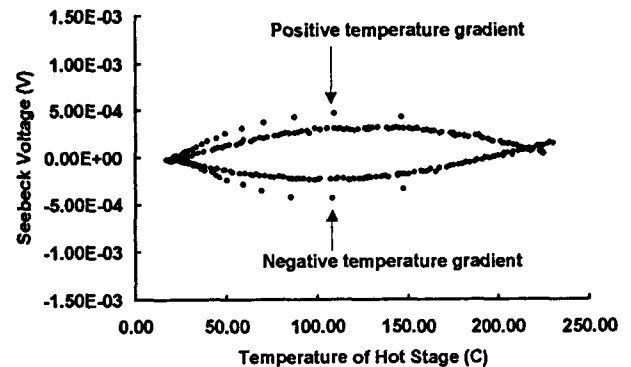


Figure 14. Seebeck voltage of bilayer film consisting of 64 angstroms of $\text{Bi}_{0.9}\text{Sb}_{0.1}$ and 115 angstroms of $\text{PbTe}_{0.8}\text{Se}_{0.2}$. The temperature of the cold stage was maintained at approximately 20°C .

This film has a very unusual non-linear voltage-temperature curve. As the film was heated, the differential voltage first increased to a maximum and then fell to zero. This is indicative of either a semiconductor-to-metal transition, or a transition from n-type to p-type behavior. The Seebeck coefficient near ambient temperature is only $-4 \mu\text{V/K}$. Clearly, reduced dimensionality has a profound effect on the observed Seebeck voltage. This observation supports the hypothesis that

improved conduction in ultra-thin $\text{Bi}_{0.9}\text{Sb}_{0.1}$ layers is due to ambipolar doping by adjacent $\text{PbTe}_{0.8}\text{Se}_{0.2}$ layers. Such doping would degrade the Seebeck coefficient, as it does in bulk thermoelectric materials. The Seebeck voltage for a multilayer film made by depositing alternating $\text{Bi}_{0.9}\text{Sb}_{0.1}$ and $\text{PbTe}_{0.8}\text{Se}_{0.2}$ layers onto an ambient-temperature, single-crystal sapphire substrate is shown in Fig. 15.

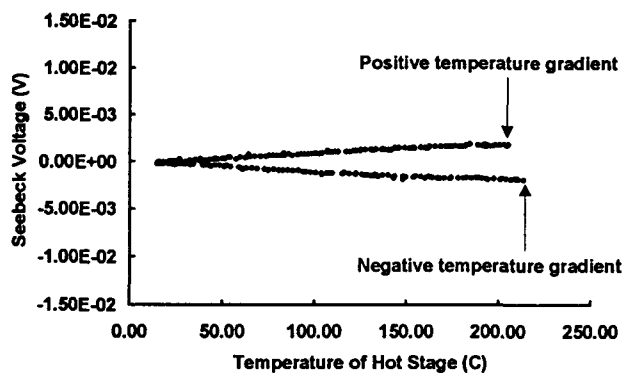


Figure 15. Seebeck voltage of multilayer film consisting of alternating layers of $\text{Bi}_{0.9}\text{Sb}_{0.1}$ and $\text{PbTe}_{0.8}\text{Se}_{0.2}$ on a single-crystal sapphire substrate. The temperature of the cold stage was maintained at approximately 20°C.

Layers of $\text{Bi}_{0.9}\text{Sb}_{0.1}$ were 143 angstroms thick, layers of $\text{PbTe}_{0.8}\text{Se}_{0.2}$ were 115 angstroms thick, and the total film thickness was approximately 17,000 angstroms. Reduced dimensionality also has a profound effect on the observed Seebeck voltages of multilayer films. The Seebeck coefficient based upon these data is only $-12 \mu\text{V/K}$. This observation also supports the hypothesis that enhanced conduction in ultra-thin $\text{Bi}_{0.9}\text{Sb}_{0.1}$ layers is due to ambipolar doping by adjacent $\text{PbTe}_{0.8}\text{Se}_{0.2}$ layers. Unlike the bilayer film with reduced dimensionality, there is no indication that the multilayer undergoes a temperature-induced n-to-p transition.

Early Attempts to Synthesize Thermoelectric Quantum Wells

$\text{Bi}_2\text{Te}_3/\text{B}_4\text{C}$ System. Initially, we attempted to prepare multilayers from Bi_2Te_3 , a well known, low-temperature thermoelectric material [15-18]. We made a number of unsuccessful attempts with dual-magnetron sputtering to deposit thin layers of Bi_2Te_3 , separated by a variety of barrier materials. Eventually, some degree of success was achieved by using B_4C as a barrier layer. These films were characterized by X-ray diffraction (XRD), transmission electron microscopy (TEM), and selected-area electron diffraction. The structure of the film was disappointing. The B_4C layer was virtually amorphous, while the Bi_2Te_3 was polycrystalline. Data indicated the presence of two crystalline phases, rhombohedral and rock-salt structures, respectively. Interfaces were unusually rough. As expected from the structural characterization, initial measurements of the Seebeck coefficient and electrical conductivity between ambient temperature and 100°C were disappointing. For example, a film with a total thickness of approximately 6,900 angstroms and 235 angstrom layer pairs had an electrical resistivity of 38 $\text{m}\Omega\text{-cm}$ and a Seebeck coefficient of $-480 \mu\text{V/K}$ near ambient temperature. The n-type behavior of this film is surprising and may be due to the presence of the rock-salt phase. These

measured properties are poor in comparison to those published for single crystals of Bi_2Te_3 at 300 K, which are 2 $\text{m}\Omega\text{-cm}$ and $+220 \mu\text{V/K}$, respectively [19]. Carrier transport in the imperfect $\text{Bi}_2\text{Te}_3/\text{B}_4\text{C}$ multilayer was probably limited by scattering and interfacial trapping.

$\text{Si}_8\text{Ge}_{20}/\text{Si}$ System. It may be possible to achieve high ZT with $\text{Si}_8\text{Ge}_{20}/\text{Si}$ heterostructures synthesized with molecular beam epitaxy (MBE). This heterostructure system is of interest since $\text{Si}_8\text{Ge}_{20}$ is the preferred thermoelectric material for high-temperature applications [20-22]. These factors prompted us to use dual-magnetron sputtering to synthesize $\text{Si}_8\text{Ge}_{20}/\text{Si}$ multilayers by alternating heavily doped, n-type $\text{Si}_8\text{Ge}_{20}$ and lightly doped Si. However, these results will not be discussed here since they are discussed in detail elsewhere [18, 23].

Summary

We have successfully synthesized $\text{Bi}_{0.9}\text{Sb}_{0.1}/\text{PbTe}_{0.8}\text{Se}_{0.2}$ single-layer, bilayer, and multilayer films with the dimensions of two-dimensional quantum wells. Layers are crystalline with a preferred orientation. Seebeck coefficients and electrical conductivities have been evaluated from ambient temperature to 200°C. Reduced dimensionality enhanced electrical conductivity of the $\text{Bi}_{0.9}\text{Sb}_{0.1}$ quantum well layer, but at the expense of the Seebeck coefficient. Ambipolar doping of the two-dimensional quantum wells by adjacent barrier layers may be hurting the overall thermoelectric performance. The thick $\text{Bi}_{0.9}\text{Sb}_{0.1}/\text{PbTe}_{0.8}\text{Se}_{0.2}$ bilayer has a much higher power factor than the $\text{Bi}_{0.9}\text{Sb}_{0.1}$ single-layer. This is probably due to the ability of the $\text{PbTe}_{0.8}\text{Se}_{0.2}$ cap to prevent any oxidation of the underlying $\text{Bi}_{0.9}\text{Sb}_{0.1}$.

Acknowledgments

Funding for this project was provided by W. Polansky and D. Barney of the United States Department of Energy (U.S. DOE) Office of Basic Energy Sciences (OBES). Contributions by P. Ramsey, W. Bell, D. Makowiecki, M. Olsen, M. Wall, A. Jankowski, R. Van Konynenburg, L. Newkirk, J. Wadsworth, and C. Gatrousis are gratefully acknowledged. This work was done under the auspices of the U.S. DOE by Lawrence Livermore National Laboratory under Contract No. W-7405-Eng-48.

References

1. Goldsmid, H. J., *Thermoelectric Refrigeration*, Plenum Press, New York, NY, 1964.
2. Egli, P. H., *Thermoelectricity*, John Wiley and Sons, New York, NY, 1958.
3. Vining, C. B., "Thermoelectric Limit $ZT \sim 1$: Fact or Artifact," presented at the XIth Intl. Conf. Thermoelectrics, K. R. Rao, Ed., Univ. Texas, Arlington, TX, Oct. 7-9, 1992.

4. Cornish, A. J., "Arrays of Inorganic Semiconducting Compounds," *J. Electrochem. Soc.* 106 8, 685-689 (1959).
5. Hicks, L. D., Dresselhaus, M.S., "Thermoelectric Figure of Merit of a One-Dimensional Conductor," *Phys. Rev. B* 47 24, 16 631-634 (1993).
6. Hicks, L. D., Dresselhaus, M.S., "Effect of Quantum-Well Structures on the Thermoelectric Figure of Merit," *Phys. Rev. B* 47 19, 12 727-731 (1993).
7. Hicks, L. D., Dresselhaus, M. S., "BiSb/PbTeSe Superlattices as a New Thermoelectric Cooling Material: Optimization of the Figure of Merit," unpublished report, March 15, 1993.
8. Hicks, L. D., Dresselhaus, M. S., "The Effects of Quantum Well Structures on the Thermoelectric Figure of Merit," presented at the 1st Natl. Thermogenic Cooler Conf., Center for Night Vision and Electro-Optics, U.S. Army, Ft. Belvoir, VA, 1992.
9. Harman, T. C., "PbTeSe/BiSb Short Period Superlattice as a New Thermoelectric Cooling Material," presented at the 1st Natl. Thermogenic Cooler Conf., Center for Night Vision and Electro-Optics, U.S. Army, Ft. Belvoir, VA, 1992.
10. Barbee, T. W., Jr., "Synthesis of Multilayer Structures by Physical Vapor Deposition Techniques," in *Synthetic Modulated Structures*, Chang, L. L., Giessen, B. C., Eds., Academic Press, Orlando, FL, 1985.
11. Barbee, T. W., Jr., "Multilayer Structures: Atomic Engineering in It's Infancy," in *Physics, Fabrication and Application of Multilayer Structures*, Dhez, P., Weisbach, C., Eds., Plenum Press, New York, NY, 1988.
12. Jankowski, A., Makowiecki, D., "W/B4C Multilayer X-Ray Mirrors," *Optical Engineering* 30 12, 2003 (1991).
13. Jankowski, A., Foreman, R., Makowiecki, D., "Fabrication of Advanced X-Ray Optics with Magnetron Mini-Source Arrays," in *SPIE Conf. Proc. Multilayer Optics for Advanced X-Ray Applications* 14, 1547 (1991).
14. N. A. Sidorenko, A. B. Mosolov, "Cryogenic Thermoelectric Coolers with Passive High-T_c Superconducting Legs," presented at the XI International Conference on Thermoelectrics, University of Texas, Arlington, October 7-9, 1992.
15. Farmer, J. C., et al., "Thermoelectric Materials with Exceptional Figures of Merit," in *Chemistry and Materials Science Progress Report, Weapons-Supporting Research and Laboratory Directed Research and Development, First Half, FY 1993*, UCID-20622-93-1, July, 1993, pp. 51-52.
16. Farmer, J. C., Barbee, T. W., Foreman, R. J., Summers, L. J., "Deposition and Evaluation of Multilayer Thermoelectric Films," presented at the 185th Electrochem. Soc. Meeting, San Francisco, CA, May 22-27, 1994; in *Proc. Symposium on Microstructures and Microfabricated Systems*, Electrochem. Soc., Pennington, NJ, 1994, Vol. 94-14, pp. 231-242; in *Extended Abstracts*, Vol. 94-1, pp. 1661-62.
17. Farmer, J. C., Ghamaty, S., Elsner, B., "Synthesis and Evaluation of Novel Thermoelectric Thin Films," presented at the Symposium on Materials Synthesis and Characterization, Division of Industrial and Engineering Chemistry, 207th Meeting of the American Chemical Society, San Diego, CA, March 13-17, 1994.
18. Farmer, J. C., et al., "Multilayer Thermoelectric Films: A Novel Approach for Achieving Exceptional Figures of Merit," 1993-94 Annual Report, Chemistry and Materials Science Department, Lawrence Livermore National Laboratory, in preparation.
19. Hyun, D-B., Ha, H-P., Shim, J-D., "Electrical and Thermoelectric Properties of Bi₂Te₃-Bi₂Se₃ Single Crystals," in *Proc. XIth Intl. Conf. Thermoelectrics*, K. R. Rao, Ed., Univ. Texas, Arlington, TX, Oct. 7-9, 1992.
20. Wood, C., "Materials for Thermoelectric Energy Conversion," *Rep. Prog. Phys.* 51, 459-539 (1988).
21. Vining, C. B., "A Model for the High-Temperature Transport Properties of Heavily Doped N-Type Silicon-Germanium Alloys," *J. Appl. Phys.* 69 1, 331-341 (1991).
22. Slack, G. A., Hussain, M. A., "The Maximum Possible Conversion Efficiency of Silicon-Germanium Thermoelectric Generators," *J. Appl. Phys.* 70 5, 2694-2718 (1991).
23. Elsner, N. B., et al., presented at this conference.